Role of Pr Segregation in Acceptor-State Formation at ZnO Grain Boundaries

Yukio Sato,[1] James P. Buban,[2] Teruyasu Mizoguchi,[2] Naoya Shibata,[2] Masatada Yodogawa,[1] Takahisa Yamamoto,[1] and Yuichi Ikuhara[2,*]

[1]*Department of Advanced Materials Science, The University of Tokyo, 5-1-5 Kashiwanoha, Kashiwa, Chiba 277-8561, Japan*
[2]*Institute of Engineering Innovation, The University of Tokyo, 2-11-16 Yayoi, Bunkyo, Tokyo 113-8656, Japan*
(Received 28 March 2006; published 5 September 2006)

The role of Pr doping on double Schottky barrier formations at ZnO single grain boundaries was investigated by the combination of current-voltage measurements, atomic-resolution *Z*-contrast scanning transmission electron microscopy, and first-principles calculations. Although Pr segregated to the specific atomic site along the boundaries, it was found not to be the direct cause of nonlinear current-voltage properties. Instead, under appropriate annealing conditions, Pr enhances formations of acceptor-type native defects that are essential for the creation of double Schottky barriers in ZnO.

DOI: 10.1103/PhysRevLett.97.106802 PACS numbers: 73.20.At, 61.72.Ji, 61.72.Mm, 68.37.Lp

Electroceramics such as ZnO, $BaTiO_3$, and $SrTiO_3$ are utilized in a broad range of electronic devices [1–6]. In such electroceramics, the unique properties originate from electrostatic potential barriers [i.e., double Schottky barriers (DSBs)] formed at the grain boundaries (GBs). Because of their importance for applications, the formation mechanisms of DSBs have been investigated over several decades [1–9]. The DSB formation is thought to be strongly dominated by atomic-scale factors, such as the GB atomic structure, dopants segregation, and/or formation of native defects.

ZnO is commonly used as surge-protecting devices (varistors), because they show nonlinear current-voltage (*I-V*) properties [2–6]. It has been thought that the properties result from DSB formation at the GBs [4]. The origin of the DSB is believed to be the formation of acceptor states at ZnO GBs. Since ZnO grains are *n*-type semiconductors, the acceptor states trap electrons from the adjacent grains, and as a result, DSBs are formed [3,4]. Previous reports have demonstrated that the atomic structure of the undoped GBs does not contribute to DSB formations [10–13]. On the other hand, doping of impurities like Pr or Bi is well known to be an effective method to cause nonlinear *I-V* properties [2–6]. These dopants are found to segregate to GBs [9,14,15], and the nonlinear *I-V* properties strongly depend on the amount of dopant segregation [16]. These results indicate that the dopant plays a key role for the formation of nonlinear *I-V* properties. In addition, it has been well demonstrated that the nonlinear *I-V* properties strongly depend on the annealing conditions, such as annealing time, atmosphere, and cooling rate [7,17]. As there is a strong correlation of the concentration of native defects with annealing conditions, it follows that the accumulation of native defects at the GB may also play a strong role for the formation of nonlinear *I-V* properties [18]. In particular, oxygen-excess–type defects, like a ''monolayer of excess oxygen'' [7] or ''chemisorbed oxygen'' [2], have been considered to be plausible origins of the DSB. On the other hand, based on results from first-principles calculations, Carlsson *et al.* recently suggested that the ''interfacial complex'' of $Bi_{Zn} + O_i + V_{Zn}$ is the origin of the DSB. [8].

Until now, the effects of the GB atomic structure, dopants, and native defects have been often considered individually. However, in practice, these atomic-scale factors can have a complex interdependence. The GB atomic structure may change by the presence of dopant as found in MgO GBs [19], and conversely, the location and distribution of the dopants should be dependent on the GB atomic structure [16,20,21]. Additionally, native defects formations are expected to depend on the GB atomic structure and dopant segregations, and vice versa. Therefore, in the present study, we investigate in detail the relationships between these atomic-scale factors and the *I-V* properties of Pr-doped ZnO single grain boundaries to understand the origin of the acceptor states. We applied the combination of *I-V* measurements, atomic-resolution *Z*-contrast scanning transmission electron microscopy (STEM), and first-principles calculation to the single GBs. Based on these results, the ensuing discussion will focus on the role of that Pr doping plays in the DSB formation at the ZnO GB.

ZnO bicrystals with [0001] $\Sigma = 7$ symmetric tilt GBs were fabricated by hot-pressing two ZnO single crystals at 1100 °C for 10 h in air. The details of the fabrication procedures were previously described elsewhere [16]. Pr was sputtered onto one side of the single crystal before joining to ensure that Pr would segregate and be present along the GB. In this orientation, both single crystals have a common [0001] axis and the GB planes are parallel to $(12\bar{3}0)$. The Pr-doped bicrystal was cut in half to investigate the effects of different cooling processes. One half was subjected to a postanneal at 1200 °C for 10 h in air and then quenched (at the rate of about 6000 °C/h). The remaining half was cooled at a slower rate of 300 °C/h. These samples will be denoted as the ''quenched'' specimen and as the ''slowly cooled'' specimen, respectively. Subsequently, the *I-V* properties across the GBs were

measured by a dc four-probe method. The atomic structure of the GBs was investigated by a STEM (JEOL 2100F) equipped with an aberration corrector (CEOS Co.). A high-angle annular dark-field detector with an inner angle greater than 60 mrad was used. In these collection conditions, the image contrast of an atomic column in the incoherent Z-contrast image is approximately proportional to the square of the average atomic number (Z) [22]. Electron energy loss spectroscopy (EELS) was performed using a Gatan Enfina system equipped on a Topcon EM-002BF transmission electron microscope. The energy resolution at full width at half maximum was measured to be 1.6 eV.

A first-principles plane-wave pseudopotential (PWPP) calculation using the VASP code was performed to obtain atomic structures of the undoped and the Pr-doped ZnO [0001] $\Sigma = 7$ GBs and the corresponding vacancy formation energies [23]. For the exchange correlation potential, the generalized gradient approximation was employed [24] and a plane-wave cutoff of 400 eV was used, as we found that the difference in GB energy was only 14 meV when using a plane-wave cutoff of 500 eV. In our previous study, atomic structure for the undoped ZnO [0001] $\Sigma = 7$ GB was calculated by using a static lattice method [13], and the obtained supercells were again optimized by the PWPP method. Supercells contain approximately 150 atoms and have two equivalent GBs. Numerical integrations over the Brillouin zone were performed only at the Γ-point because of the large size of supercells. All atoms in the supercells were optimized until the residual forces were less than 0.1 eV/Å. In this study, the formation energies of V_{Zn} and O_i defects are calculated because it is thought that these were the most likely defect types to form acceptor states in ZnO GBs [2,7–9,18,25–27]. The formation energies of V_{Zn} and O_i($E[V_{\mathrm{Zn}}]$ and $E[\mathrm{O}_i]$) are calculated by the following formulas:

$$E[V_{\mathrm{Zn}}] = E_{\mathrm{tot}}[\mathrm{defect}] - E_{\mathrm{tot}}[\mathrm{host}] + \mu_{\mathrm{Zn}} - 2\mu_e, \quad (1)$$

$$E[\mathrm{O}_i] = E_{\mathrm{tot}}[\mathrm{defect}] - E_{\mathrm{tot}}[\mathrm{host}] - \mu_{\mathrm{O}} - 2\mu_e. \quad (2)$$

Here, $E_{\mathrm{tot}}[\mathrm{defect}]$ and $E_{\mathrm{tot}}[\mathrm{host}]$ are the total energies of the supercells with and without the point defects, and μ_{Zn}, μ_{O}, and μ_e are the chemical potentials of Zn, O, and the electron (i.e., the Fermi energy), respectively. At the oxygen-rich condition, μ_{O} is equal to μ_{O} in a O_2 molecule, and $\mu_{\mathrm{Zn}} = \mu_{\mathrm{ZnO}} - \mu_{\mathrm{O}}$, where μ_{ZnO} is the chemical potential of the ZnO perfect crystal. In the present calculations, we assumed that μ_e is 1 eV, which corresponds to n-type ZnO [27]. The charge states of V_{Zn} and O_i are assumed to be -2, as these charge states are reported to be stable under the n-type and oxygen-rich conditions [27].

Figure 1 shows the I-V properties across the GBs in both the slowly cooled and the quenched specimens. The I-V properties of both specimens are significantly different, depending on the annealing conditions. The quenched specimens show linear I-V properties, whereas the slowly cooled specimens exhibit nonlinear I-V properties that are considered to be due to DSB formation at the GB. This indicates that the DSB formation is more enhanced during the cooling rather than during annealing at high temperature. Therefore, important changes in one or more of the atomic-scale factors (GB atomic structure, Pr segregations, or native defects accumulations) must occur during the cooling.

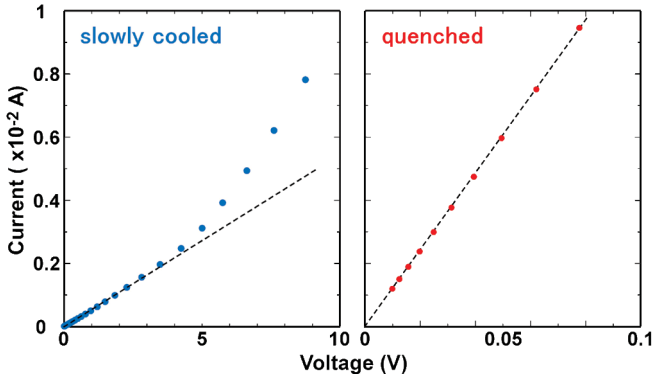

FIG. 1 (color). The I-V properties across the GBs in slowly cooled and quenched specimens. Linear properties are extrapolated by dotted lines. The I-V property of the quenched specimen is linear, while that of the slowly cooled one is nonlinear.

Figure 2 shows a typical Z-contrast STEM image of the GBs. In the image, atomic columns of very bright intensity are found to be present periodically along the GB. The intensity profile along the line A-B is shown in the inset, in which much brighter spots exhibit higher intensity than the others. Since the atomic number of Pr (59) is larger than that of Zn (30), the very bright spots indicate the presence of Pr. Pr is found to be localized at the GB core; this dopant distribution is commonly found in both the slowly cooled and the quenched specimens.

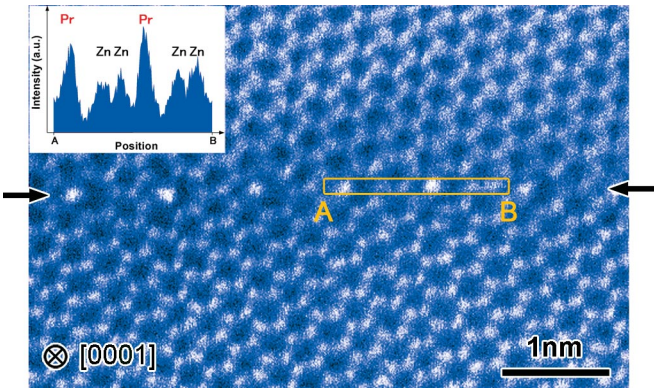

FIG. 2 (color). A typical Z-contrast STEM image of the Pr-doped ZnO [0001] $\Sigma = 7$ GBs. The position of the GB plane is indicated by the arrows, and the inset shows the intensity profile along the GB (A-B). Very bright spots appear along the GB, indicating the presence of Pr.

Figures 3(a) and 3(b) show typical atomic structures found in the GBs of the slowly cooled and the quenched specimens, respectively. Both images show that the GBs are atomically sharp, with no secondary phases or amorphous regions present. Furthermore, neither a monolayer of excess oxygen nor chemisorbed oxygen [2,7] could be observed even in the slowly cooled boundary with the nonlinear I-V characteristics. Moreover, it was found that both the slowly cooled and the quenched specimens have very similar atomic structures. Thus, the change of annealing conditions seems not to affect the basic GB atomic structures. Comparing the atomic structure of the Pr-doped $\Sigma = 7$ GBs with those for the undoped $\Sigma = 7$ GB (see Ref. [13]) suggests that Pr segregates to specific atomic columns that are periodic along the GB. First-principles calculation will later reveal that Pr does indeed substitute for Zn at the GB. Figure 3(c) shows the EELS Pr-$M_{4,5}$ edge obtained from both the GBs. Both spectra show the appearance of a shoulder at the left side of the second peak (M_4 edge) as indicated with hatches. This feature shows that Pr is identified to be in the 3+ state [28]. As the substitution of Pr^{3+} for Zn^{2+} in ZnO would produce donor states rather than acceptor states, Pr itself cannot be the direct cause of DSB formation at the GB. Here, it is worth noting that, using EELS, we also investigated O-K edges and Zn-L edges from both the slowly cooled and the quenched GBs. However, neither the fine structure nor the Zn-O ratio showed any major differences.

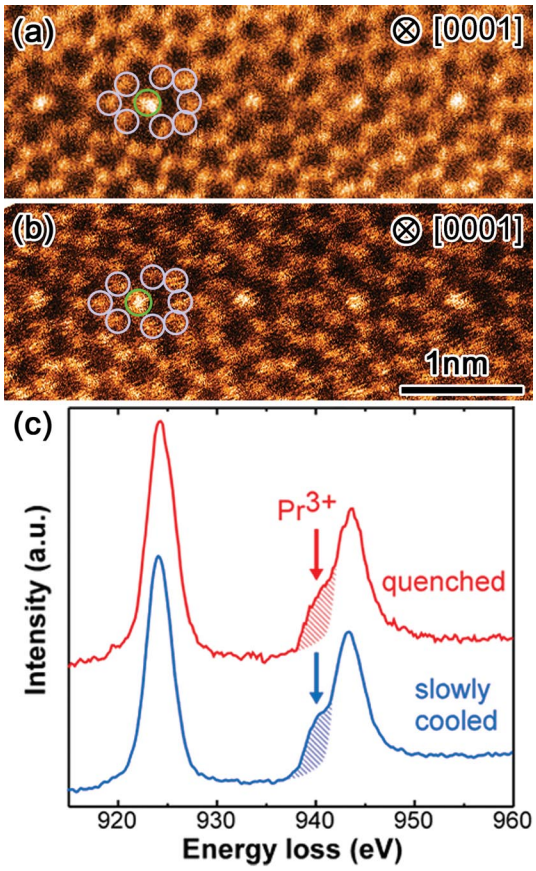

FIG. 3 (color). Magnified Z-contrast images of the GBs in (a) the slowly cooled specimen and (b) the quenched specimen. Positions of atomic columns at the GB core are superimposed by light blue and green circles. (From [0001] incident direction, Zn and O are projected in the same column. Green circles indicate atomic columns including Pr.) (c) Pr-$M_{4,5}$ edge EELS spectra obtained from both the GBs. Hatches and arrows show the shoulders appearing at left side of the second peaks.

Figures 4(a) and 4(b) show the stable atomic structures of the undoped and Pr-doped GBs obtained by the PWPP calculation. The location of Pr was determined by calculating the substitution energy of Pr for Zn. It was found that the calculated atomic structures of the GBs match well with the STEM image. (See Ref. [13] for the undoped case.) The formation energies of V_{Zn} defects at sites 1 and 2 and O_i defects at sites 3 and 4 [shown in Figs. 4(a) and 4(b)] were also calculated, and the results are summarized in Fig. 4(c). For both the undoped and the Pr-doped cases, the V_{Zn} defect is found to be more stable than the O_i defect, indicating that the V_{Zn} defect is the dominant species among the acceptor-state forming point defects. Another key feature is that Pr-doping lowers the formation energies of those defects mentioned above. This strongly indicates that Pr plays an important role of promoting the point defects formations, particularly the V_{Zn} defect.

Recently, Carlsson *et al.* reported a theoretical study of Bi segregation in a ZnO GB [8]. Their first-principles calculation revealed that the formation of a defect complex

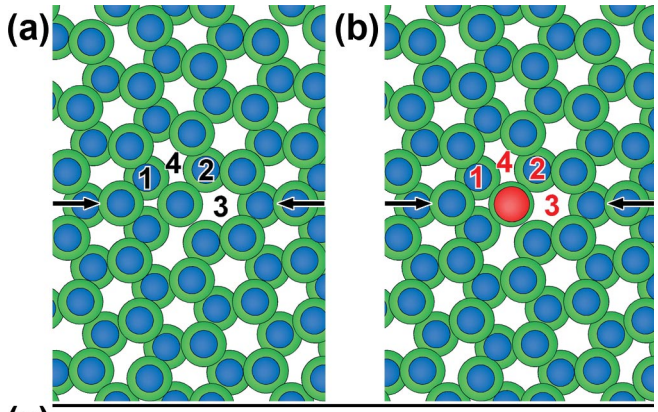

Atomic site (species)	Formation energy (eV)	
	Undoped	Pr doped
1 (V_{Zn})	0.9	0.4
2 (V_{Zn})	1.4	1.0
3 (O_i)	2.9	2.1
4 (O_i)	3.0	2.1

FIG. 4 (color). The atomic structures used in the first-principles calculation for (a) the undoped and (b) the Pr-doped GBs. Arrows indicate the positions of the GBs. Blue, green, and red circles denote Zn, O, and Pr, respectively. V_{Zn} or O_i was introduced at four different sites indicated by 1–4 for both GBs. (c) Formation energies of V_{Zn} or O_i at sites 1–4 for both GBs.

of Bi and native defects ($Bi_{Zn} + V_{Zn} + O_i$) is energetically favorable at the GB in oxygen-rich conditions. They suggested that these complexes would create the localized GB acceptor states essential for DSB formation. Our experimental and theoretical results clearly show that Pr substitutes only for specific Zn sites along the GB and that they promote the formation of V_{Zn} and O_i in their vicinity. These findings are basically consistent with the Bi case, but our *I-V* property measurement indicates the importance of the annealing processes for the actual DSB formation. We found experimentally that the *I-V* properties are strongly dependent on the different thermal histories, whereas the atomic structure, Pr segregation, and the Pr valence state are found to be independent of the annealing conditions. These results suggest that the native defects are indeed the most plausible origin of DSBs, but their formation should be strongly affected by the annealing processes. Carlsson *et al.* suggested that the complexes of Bi and native defects are initially formed during sintering and subsequently frozen in during the cooling processes. In this scenario, the DSB would already be formed during the high-temperature anneal and kept constant during cooling, which, however, is not consistent with the present Pr-doped case. We think that the native defects are likely to accumulate at GBs during the cooling process, and that further investigations are needed for this issue. For example, concentrations and distributions of vacancies may be observed using Cs-corrected TEM [29]. However, the fundamental effect of Pr doping is to enhance the native defect formations under appropriate conditions, which may be also applicable to other dopant systems.

In summary, investigations of ZnO bicrystals were used to identify the effect of Pr doping on the nonlinear *I-V* properties across GBs. It was found that Pr itself is not the direct cause of the property, but with the suitable annealing conditions, Pr enhances the DSB formation at the GBs. Atomic-resolution *Z*-contrast images clearly revealed that Pr segregates only to the specific atomic sites along the GBs. According to the first-principles calculations based on the obtained structure, it was found that the Pr enhances the formation of acceptor-type native defects (V_{Zn} and O_i), which are essential for DSB formations. This is believed to be the fundamental role of Pr, and the effect is likely to be enhanced under suitable annealing conditions.

A part of this study was supported by the Japan Society for the Promotion of Science (JSPS). Both Y. S. and J. P. B. received additional support from JSPS.

*To whom correspondence should be addressed.
Electronic address: ikuhara@sigma.t.u-tokyo.ac.jp

[1] W. Heywang, J. Am. Ceram. Soc. **47**, 484 (1964).
[2] D. R. Clarke, J. Am. Ceram. Soc. **82**, 485 (1999).
[3] F. Greuter and G. Blatter, Semicond. Sci. Technol. **5**, 111 (1990).
[4] G. E. Pike and C. H. Seager, J. Appl. Phys. **50**, 3414 (1979).
[5] M. Matsuoka, Jpn. J. Appl. Phys. **10**, 736 (1971).
[6] K. Mukae, K. Tsuda, and I. Nagasawa, Jpn. J. Appl. Phys. **16**, 1361 (1977).
[7] F. Stucki and F. Greuter, Appl. Phys. Lett. **57**, 446 (1990).
[8] J. M. Carlsson, H. S. Domingos, P. D. Bristowe, and B. Hellsing, Phys. Rev. Lett. **91**, 165506 (2003).
[9] Y. Sato, T. Mizoguchi, F. Oba, M. Yodogawa, T. Yamamoto, and Y. Ikuhara, Appl. Phys. Lett. **84**, 5311 (2004).
[10] J. M. Carlsson, B. Hellsing, H. S. Domingos, and P. D. Bristowe, J. Phys. Condens. Matter **13**, 9937 (2001).
[11] F. Oba, S. R. Nishitani, H. Adachi, I. Tanaka, M. Kohyama, and S. Tanaka, Phys. Rev. B **63**, 045410 (2001).
[12] Y. Sato, F. Oba, T. Yamamoto, Y. Ikuhara, and T. Sakuma, J. Am. Ceram. Soc. **85**, 2142 (2002).
[13] Y. Sato, T. Mizoguchi, F. Oba, M. Yodogawa, T. Yamamoto, and Y. Ikuhara, J. Mater. Sci. **40**, 3059 (2005).
[14] K. Kobayashi, O. Wada, M. Kobayashi, and Y. Takada, J. Am. Ceram. Soc. **81**, 2071 (1998).
[15] W. D. Kingery, J. B. V. Sande, and T. Mitamura, J. Am. Ceram. Soc. **62**, 221 (1979).
[16] Y. Sato, F. Oba, M. Yodogawa, T. Yamamoto, and Y. Ikuhara, J. Appl. Phys. **95**, 1258 (2004).
[17] E. Olsson and G. L. Dunlop, J. Appl. Phys. **66**, 3666 (1989).
[18] G. D. Mahan, J. Appl. Phys. **54**, 3825 (1983).
[19] Y. Yan, M. F. Chisholm, G. Duscher, A. Maiti, S. J. Pennycook, and S. T. Pantelides, Phys. Rev. Lett. **81**, 3675 (1998).
[20] J. P. Buban, K. Matsunaga, J. Chen, N. Shibata, W. Y. Ching, T. Yamamoto, and Y. Ikuhara, Science **311**, 212 (2006).
[21] R. F. Klie, J. P. Buban, M. Varela, A. Franceschetti, C. Jooss, Y. Zhu, N. D. Browning, S. T. Pantelides, and S. J. Pennycook, Nature (London) **435**, 475 (2005).
[22] S. J. Pennycook, in *Advances in Imaging and Electron Physic*, edited by P. G. Merli, G. Calestani, and M. Vittori-Antisari (Academic Press, London, 2002), Vol. 123, p. 173.
[23] G. Kresse and J. Furthmüller, Phys. Rev. B **54**, 11 169 (1996).
[24] J. P. Perdew, J. A. Chevary, S. H. Vosko, K. A. Jackson, M. R. Pederson, D. J. Singh, and C. Fiolhais, Phys. Rev. B **46**, 6671 (1992).
[25] A. F. Kohan, G. Ceder, D. Morgan, and C. G. Van de Walle, Phys. Rev. B **61**, 15 019 (2000).
[26] S. B. Zhang, S.-H. Wei, and A. Zunger, Phys. Rev. B **63**, 075205 (2001).
[27] F. Oba, S. R. Nishitani, S. Isotani, H. Adachi, and I. Tanaka, J. Appl. Phys. **90**, 824 (2001).
[28] Z. Hu, G. Kaindl, H. Ogasawara, A. Kotani, and I. Felner, Chem. Phys. Lett. **325**, 241 (2000).
[29] C. L. Jia, M. Lentzen, and K. Urban, Science **299**, 870 (2003).